Article

Electrical Properties of Membrane Phospholipids in Langmuir Monolayers

Anna Chachaj-Brekiesz [1] **, Jan Kobierski** [2] **, Anita Wnętrzak** [1] **and Patrycja Dynarowicz-Latka** [1,*]

[1] Faculty of Chemistry, Jagiellonian University, Gronostajowa 2, 30-387 Kraków, Poland; anna.chachaj@uj.edu.pl (A.C.-B.); anita.wnetrzak@uj.edu.pl (A.W.)

[2] Department of Pharmaceutical Biophysics, Faculty of Pharmacy, Jagiellonian University Medical College, Medyczna 9, 30-688 Kraków, Poland; jan.kobierski@uj.edu.pl

[*] Correspondence: ucdynaro@cyf-kr.edu.pl

Abstract: Experimental surface pressure (π) and electric surface potential (ΔV) isotherms were measured for membrane lipids, including the following phosphatidylcholines (PCs)—1,2-dipalmitoyl-sn-glycero-3-phosphocholine (DPPC); 1,2-distearoyl-sn-glycero-3-phosphocholine (DSPC); 1,2-diarachidoyl-sn-glycero-3-phosphocholine (DAPC); and 1,2-dioleoyl-sn-glycero-3-phosphocholine (DOPC). In addition, other phospholipids, such as phosphatidylethanolamines (represented by 1,2-dipalmitoyl-sn-glycero-3-phosphoethanolamine (DPPE)) and sphingolipids (represented by N-(hexadecanoyl)-sphing-4-enine-1-phosphocholine (SM)) were also studied. The experimental apparent dipole moments (μ_A^{exp}) of the abovementioned lipids were determined using the Helmholtz equation. The particular contributions to the apparent dipole moments of the investigated molecules connected with their polar ($\mu_\perp^p$) and apolar parts ($\mu_\perp^a$) were theoretically calculated for geometrically optimized systems. Using a three-layer capacitor model, introducing the group's apparent dipole moments (calculated herein) and adopting values from other papers to account for the reorientation of water molecules ($\mu_\perp^w / \varepsilon_w$), as well as the for the local dielectric permittivity in the vicinity of the polar (ε_p) and apolar (ε_a) groups, the apparent dipole moments of the investigated molecules were calculated (μ_A^{calc}). Since the comparison of the two values (experimental and calculated) resulted in large discrepancies, we developed a new methodology that correlates the results from density functional theory (DFT) molecular modeling with experimentally determined values using multiple linear regression. From the fitted model, the following contributions to the apparent dipole moments were determined: $\mu_\perp^w / \varepsilon_w = -1.8 \pm 1.4\ D$; $\varepsilon_p = 10.2 \pm 7.0$ and $\varepsilon_a = 0.95 \pm 0.52$). Local dielectric permittivity in the vicinity of apolar groups (ε_a) is much lower compared to that in the vicinity of polar moieties (ε_p), which is in line with the tendency observed by other authors studying simple molecules with small polar groups. A much higher value for the contributions from the reorientation of water molecules ($\mu_\perp^w / \varepsilon_w$) has been interpreted as resulting from bulky and strongly hydrated polar groups of phospholipids.

Keywords: Langmuir monolayers; electric surface potential; dipole moments; phospholipids

1. Introduction

The Langmuir monolayers formed by insoluble amphiphiles at the free water surface have mainly been analyzed using the classical method based on recording surface pressure (π)–area (A) isotherms, which enables researchers to monitor changes of the physical state of film molecules upon compression [1]. Their visualization is possible with microscopic methods like Brewster angle microscopy [2] and fluorescence microscopy [3]. Changes in the electric potential (ΔV), which provide important information on the orientation of molecules at the surface, are performed less frequently. Such measurements complement the characterization of the film's electrical properties (including dipole moments and dielectric permittivity), which play an important role in many intermolecular interactions.

Their analysis provides the basis for an insight into the understanding of biomolecular processes in membranes.

A Langmuir monolayer can be considered as an array of electric dipoles of film-forming molecules situated at the air/water interface. Of particular interest are phospholipid monolayers, which provide a simplified, two-dimensional membrane model that is suitable for studying interactions [4]. Particularly important are those between the polar groups of film molecules and substances dissolved in the subphase (ions and soluble biomolecules). During interactions, the electrical surface potential of the monolayer can be decreased or increased. The measurements of such modifications are of great value as they can be used to screen drugs and check their effectiveness [5–8].

The experimental surface potential changes of a monolayer have usually been interpreted in the terms of so-called effective dipole moments ($\mu_\perp$). In the simplest approach, derived from the parallel plate condenser model [9], ΔV is expressed by the Helmholtz equation:

$$\Delta V = \frac{\mu_\perp}{A \varepsilon \varepsilon_0} \tag{1}$$

where ε is the dielectric permittivity of the film, ε_0 is the dielectric permittivity of the vacuum, $\mu_\perp$ is the normal (to the interface) component of the dipole moment of the film molecule at the interface (note that this is different from the molecular dipole moment of the free molecule) and A is the average area occupied by the molecule at the surface ($A = 1/N$, where N is the total number of molecules at 1 cm^2 of the surface). The above equation applies to un-ionized molecules. For ionized ones, the double layer potential (ψ_0) must be taken into account [9,10]. The main problem in Equation (1) is the unknown value of the permittivity of the film, ε. One of the approaches assumes that $\varepsilon = 1$, either because molecules are considered as isolated entities or because of the lack of a known value [10], however, this can be assumed only for gaseous films. Some authors have claimed that a value $5 < \varepsilon < 10$ should be used [11]. Others suggest that for condensed monolayers, ε can be taken as 2, which is the dielectric permittivity of hydrocarbons [12]. In another approach, the unknown value of ε has been included in the so-called "apparent dipole moment" of a film molecule, $\mu_A = \frac{\mu_\perp}{\varepsilon}$ [13]. μ_A can be easily determined from the experimental values of ΔV as a function of A. Apart from the Helmholtz model, other approaches have been suggested in order to interpret surface potential changes (reviewed in [14,15]). A frequently used model was provided by Demchak and Fort [16], which treats the monolayer as a three-layer capacitor. In this model, the effective dipole moment of a film molecule can be divided into the contributions from the reorientation of water molecules in the monolayer, the polar and apolar part of the film molecule ($\mu_\perp^w$, $\mu_\perp^p$ and $\mu_\perp^a$, respectively), divided by their local dielectric permittivities:

$$\Delta V = \frac{1}{A \varepsilon_0} \left(\frac{\mu_\perp^w}{\varepsilon_w} + \frac{\mu_\perp^p}{\varepsilon_p} + \frac{\mu_\perp^a}{\varepsilon_a} \right) \tag{2}$$

Equation (2) has been used to interpret electric surface potentials for both adsorbed [17] as well as insoluble monolayers [18]. Group dipole moments, $\mu_\perp^p$ and $\mu_\perp^a$ were calculated from bond dipole moments and angles between them, whereas local dielectric permittivities ε_a and ε_p were obtained by solving in pairs equations of type (2) for molecules having the same apolar parts and different polar parts, and vice versa, assuming that the contribution from the reorientation of water molecules ($\mu_\perp^w/\varepsilon_w$) in each pair of equations is the same. Using this procedure for adsorbed films [17] and Langmuir monolayers [18,19] formed by carboxylic acids, alcohols and their derivatives, the following values were obtained: $\varepsilon_p = 4.2$; $\varepsilon_a = 2.4$; ($\mu_\perp^w/\varepsilon_w$) = $-100 \div -200$ mD; $\varepsilon_p = 6.4$; $\varepsilon_a = 2.8$; ($\mu_\perp^w/\varepsilon_w$) = -65 mD, and $\varepsilon_p = 7.6$; $\varepsilon_a = 4.2$; ($\mu_\perp^w/\varepsilon_w$) = 25 mD, respectively. Upon analyzing surface potential changes for terphenyl derivatives [16], the following values were obtained: $\varepsilon_p = 7.6$; $\varepsilon_a = 5.3$; ($\mu_\perp^w/\varepsilon_w$) = 40 mD. Although there are some differences as regards the values of local dielectric permittivities, ε_p is always higher than ε_a. The greatest discrepancies

concern values of ($\mu_\perp^w / \varepsilon_w$), which are generally small, but their sign was determined to be positive or negative.

The history of measuring surface potentials of Langmuir films from membrane lipids is relatively long but there are many discrepancies in the reported values [20–22]. This can result from the applied approaches, laboratory procedures as well as equipment (including types of measuring electrodes used). Although nowadays this technique is routinely applied in order to analyse the electrical properties of surface films [7,8,23,24], in the literature there are results for selected, single molecules only and no systematic studies, especially for biologically important molecules, are available. The main constituent molecules of biomembranes, i.e., phospholipids, are of particular importance. Therefore, the aim of this paper was to provide the characteristics of the electrical properties of the most abundant membrane phospholipids, i.e., phosphatidylcholines (PCs), differing in acyl chain length (1,2-dipalmitoyl-sn-glycero-3-phosphocholine (DPPC); 1,2-distearoyl-sn-glycero-3-phosphocholine (DSPC); 1,2-diarachidoyl-sn-glycero-3-phosphocholin (DAPC) and unsaturation (1,2-dioleoyl-sn-glycero-3-phosphocholine (DOPC). For comparison, other phospholipids, such as phosphatidylethanolamines (represented by 1,2-dipalmitoyl-sn-glycero-3-phosphoethanolamine (DPPE) and sphingolipids (represented by N-(hexadecanoyl)-sphing-4-enine-1-phosphocholine (SM) were also investigated. The chemical structures of the studied phospholipids are shown in Figure 1. All phospholipids selected for our study have net charge zero at pH 7.
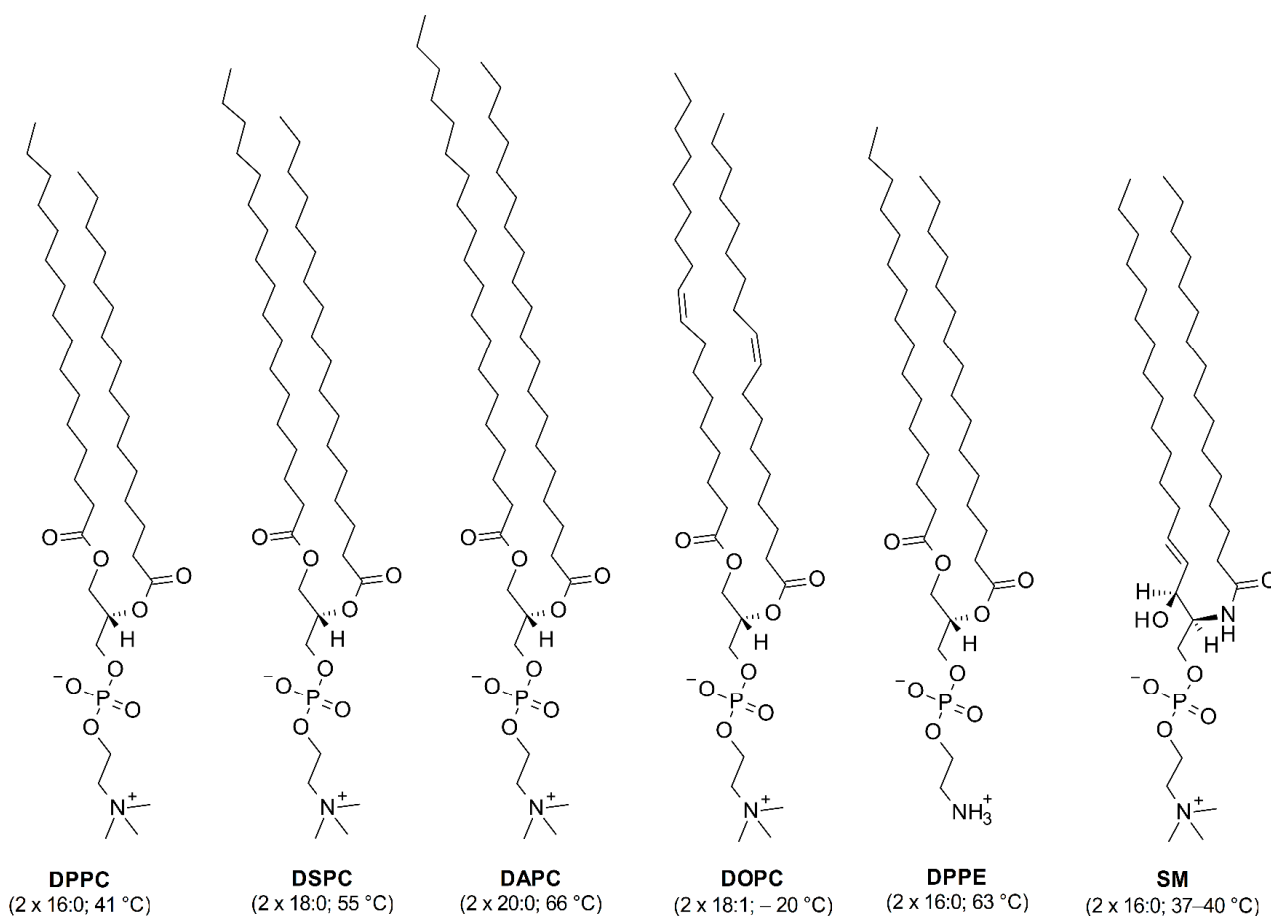

Figure 1. Chemical structures of the studied phospholipids together with acyl chain lengths. Chain melting temperatures of the hydrocarbon chains are given in parentheses. DPPC- 1,2-dipalmitoyl-sn-glycero-3-phosphocholine; DSPC- 1,2-distearoyl-sn-glycero-3-phosphocholine; DAPC -1,2-diarachidoyl-sn-glycero-3-phosphocholine; DOPC- 1,2-dioleoyl-sn-glycero-3-phosphocholine; DPPE- 1,2-dipalmitoyl-sn-glycero-3-phosphoethanolamine; SM- N-(hexadecanoyl)-sphing-4-enine-1-phosphocholine.

The theoretical models used so far for determining the apparent dipole moments and local dielectric permittivities were developed for very simple molecules such as carboxylic acids, alcohols and amines. The use of these models to determine the electrical properties of more complex molecules has not worked well. Therefore, an additional goal of our research was to develop a universal model to be used for molecules of any structure, based on density functional theory (DFT) modeling and multiple linear regression.

2. Materials and Methods

2.1. Surface Potential Measurements

DPPC (1,2-dipalmitoyl-sn-glycero-3-phosphocholine; 16:0 PC), DSPC (1,2-distearoyl-sn-glycero-3-phosphocholine; 18:0 PC), DAPC (1,2-diarachidoyl-sn-glycero-3-phosphocholine; 20:0 PC); DOPC (1,2-dioleoyl-sn-glycero-3-phosphocholine; 18:1 PC), egg SM (containing 86% of N-(hexadecanoyl)-sphing-4-enine-1-phosphocholine; 16:0 SM) and DPPE (1,2-dipalmitoyl-sn-glycero-3-phosphoethanolamine; 16:0 PE) in purities > 99% were supplied by Avanti Polar Lipids. All the investigated phospholipids (except for DOPC) were investigated below their chain melting temperatures (specified in Figure 1). Ethanol (98%) and spectral grade chloroform (stabilized with ethanol) were delivered by Sigma-Aldrich. Spreading solutions for Langmuir experiments were prepared by dissolving each compound in chloroform or chloroform:ethanol (9:1) with a typical concentration of 0.2–0.3 mg·mL^{-1}. In a standard experiment, 50–100 μL of the investigated solution was spread with a microsyringe (precise to ±2.5 μL). After spreading, the monolayers were left for 10 min for solvent evaporation before starting the compression at a barrier speed of 20 cm^2/min. Deionized ultrapure water from a Millipore system with a resistivity of 18.2 MΩ·cm, pH 7, and a surface tension of 72.8 mN/m was used as a subphase. The subphase temperature (20 °C) was controlled to within 0.1 °C using a thermostat from Julabo. Experiments were carried out with a two-barrier Langmuir 612D NIMA trough (total area 600 cm^2) placed on an antivibration table. Surface pressure was measured with an accuracy of 0.1 mN/m using a Wilhelmy plate made of chromatography paper (Whatman Chr1) as the pressure sensor. Electric surface potential measurements were performed using a Kelvin probe (model KP2, NFT) mounted on a 612D NIMA trough. The vibrating plate was located ca. 2 mm above the water surface while the reference electrode, made from platinum foil, was placed in the water subphase. The surface potential measurements were reproducible to ±15 mV and ±2 Å^2 per molecule. Experimental results of surface pressure–area and electric surface potential–area isotherms presented here are representative curves selected from at least three overlapping experiments.

2.2. Theoretical Calculations

The dipole moments and of polar $\mu_\perp^p$ and apolar $\mu_\perp^a$ parts of molecules were calculated for previously geometrically optimized systems using the Gaussian 16 software package [25]. Geometry optimization was performed by density functional theory (DFT) modeling. All calculations were performed using the B3LYP functional [26–29] with a 6-311+G(d,p) basis set [30,31] and the D3 version of Grimme's empirical dispersion with the original D3 damping function [32]. Systems were optimized with the default convergence procedures, with no Fermi broadening.

3. Results and Discussion

The results of surface pressure (π) and electric surface potential changes (ΔV) versus area per molecule (A) measurements for the investigated lipids are presented in Figures 1 and 2. Experimental π–A isotherms for all the studied phospholipids are in good agreement with those already published ([33] for DPPC, [34] for DSPC, [35] for DAPC, [36] for DOPC, [37] for DPPE and [38] for SM). Experimental ΔV − A curves can be characterized by two important parameters: critical area (A$_c$, which corresponds to the area at which ΔV is triggered off) and maximum value of surface potential (ΔV$_{max}$). The change in surface potential, observed at A$_c$ occurs at much earlier stages of monolayer compression

compared to the surface pressure lift-off area ($A_{lift-off}$) [10]. The onset areas of both surface pressure ($A_{lift-off}$) and surface potential (A_c) occur at the largest areas for the unsaturated phospholipid DOPC. This is due to the steric requirements for molecules with cis unsaturated bonds in their chains, having a coiled conformation, in contrast to saturated all-trans chains. For uncharged compounds, ΔV is approximately constant and close to zero at large areas per molecule. Upon compression, a sharp change (increase or decrease) is observed at the critical area. Changes in the slope of ΔV–A dependence reflect molecular orientation and/or conformational changes in the layer, as ΔV is proportional to the magnitude of the electrostatic field gradient normal to the subphase surface [1]. The maximum of the surface potential, ΔV_{max}, is defined as the value corresponding to the most vertical orientation of molecules, which usually coincides with the maximum condensation of the monolayer, characterized by the maximum compressibility modulus: $C_s^{-1} = -A\left(\frac{d\pi}{dA}\right)$ [39]. Finally, at a collapse point, ΔV becomes approximately constant. The maximum value of the surface potential, ΔV_{max}, is used to calculate the apparent dipole moment μ_A^{exp} of film molecules, using the following equation:

$$\mu_A^{exp} = \frac{\mu_\perp}{\varepsilon} = \varepsilon_0 \cdot A \cdot \Delta V_{max} \tag{3}$$

wherein ε_0 is the vacuum permittivity, ε is the monolayer permittivity (unknown) and A and ΔV_{max} are values extracted from experimental curves corresponding to the maximum compressibility modulus. The values of μ_A^{exp} for all the investigated phospholipids, together with other characteristic parameters for their monolayers, such as $A_{lift-off}$, A_c, ΔV_{max} and A, are summarized in Table 1.
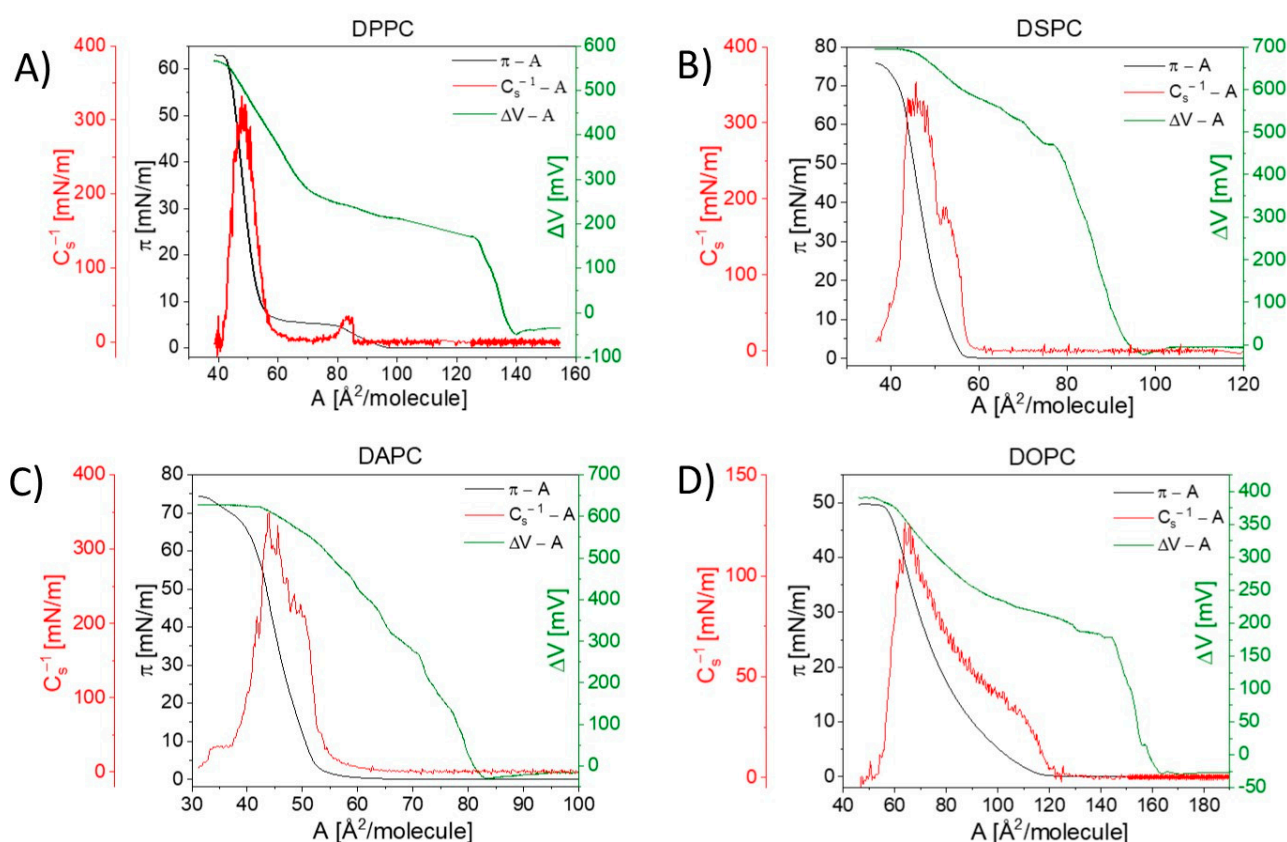

Figure 2. Electric surface potential change and surface pressure isotherms, together with calculated compressional moduli curves for selected phosphatidylcholines: (**A**) DPPC (1,2-dipalmitoyl-sn-glycero-3-phosphocholine), (**B**) DSPC (1,2-distearoyl-sn-glycero-3-phosphocholine), (**C**) DAPC (1,2-diarachidoyl-sn-glycero-3-phosphocholine) and (**D**) DOPC (1,2-dioleoyl-sn-glycero-3-phosphocholine).

Table 1. Selected data read from surface pressure–area (π–A) and electric surface potential–area (ΔV–A) experimental curves measured at 20 °C, together with experimental apparent dipole moments μ_A^{exp} values (uncertainty of $\pm\Delta\mu_A^{exp}$ was obtained by exact differential method)—explanation in the text.

Phospholipid	$A_{lift-off}$ [Å²/molecule]	A_c [Å²/molecule]	A [Å²/molecule]	ΔV_{max} [mV]	μ_A^{exp}[D]	$\pm\Delta\mu_A^{exp}$ [D]
DPPC [1]	96.2	139.0	47.8	509	0.64	0.05
DSPC [2]	57.2	96.2	45.8	684	0.83	0.05
DAPC [3]	58.5	82.6	43.7	614	0.71	0.05
DOPC [4]	116.8	162.3	64.0	358	0.61	0.04
DPPE [5]	62.2	144.2	47.7	573	0.73	0.05
SM [6]	78.3	92.9	42.0	295	0.33	0.03

[1] 1,2-dipalmitoyl-sn-glycero-3-phosphocholine; [2] 1,2-distearoyl-sn-glycero-3-phosphocholine; [3] 1,2-diarachidoyl-sn-glycero-3-phosphocholine; [4] 1,2-dioleoyl-sn-glycero-3-phosphocholine; [5] 1,2-dipalmitoyl-sn-glycero-3-phosphoethanolamine; [6] N-(hexadecanoyl)-sphing-4-enine-1-phosphocholine.

Let us first discuss the surface potential change curves recorded for phosphatidyl-choline derivatives (Figure 2), in which the length of the apolar acyl chain or unsaturation degree is varied.

The ΔV–A curve recorded for DPPC shows a characteristic sharp increase starting at the molecular area ca. 139.0 Å² from −30 to ca. 168 mV, where there is a visible inflection. Then, the surface potential rise is continued, albeit with a much smaller slope. Starting from ca. 68 Å²/molecule and 283 mV, the curve slope increases again. A similar sequence is observed in the π–A isotherm and can be attributed to a change in physical surface states in DPPC, i.e., a phase transition from a liquid-expanded (LE) to a liquid-condensed (LC) phase. As is well known, the LC state is more ordered than the LE state due to (i) closer molecular packing (resulting from the increased conformational order of hydrocarbon chains), and (ii) the smaller tilt angle of molecules in the surface layer [40]. The most condensed DPPC monolayer is characterized by a surface potential change equal to 509 mV, which is in agreement with previous studies (527 mV [23], 551 mV [24] and 544 mV [41]). Further elongation of acyl chains to 18 (DSPC) and 20 (DAPC) carbons influence the electrical properties of the formed monolayers. The critical area becomes shifted to smaller values: 96.2 and 82.6 Å²/molecule for DSPC and DAPC, respectively. This suggests that phosphatidylcholines with longer hydrocarbon chains form more tightly packed and more condensed films compared to the DPPC monolayer. The curve for DSPC is characterized by one inflection appearing at ca. 77 Å²/molecule and 466 mV, which suggests changes in molecular orientation in the monolayer (understood as a change in molecular angle in respect to the surface) [42]. On the other hand, the ΔV–A isotherm for DAPC shows a gradual rise without noticeable slope changes until the film collapse. The maximum surface potential values are equal to 684 mV and 614 mV for DSPC and DAPC, respectively. The DOPC molecule possesses one double bond in each of the octadecyl chains and can be compared to DSPC, which has hydrophobic chains of the same length, but both are saturated. As can be noticed, the ΔV–A curves of both phospholipids are characterized by the same shape (with one inflection). However, some differences should also be noted. Firstly, the critical area for DOPC is approximately 66 Å²/molecule larger as compared to DSPC. This suggests lower packing of the DOPC film, which is also confirmed by the values of the compressibility moduli. Secondly, the maximum value of the surface potential ΔV_{max} is equal to 358 mV. Since the surface potential is proportional to the component of the electrostatic field vertical to the surface, it can be concluded that DOPC acyl chains in the monolayer are more disordered in comparison to DSPC. The molecular basis of this issue is due to the presence of double bonds in the cis configuration in DOPC. The configuration of unsaturated bonds affects the conformation of entire hydrocarbon chains, causing disorders (gauche defects, etc.). In contrast, the DSPC hydrocarbon backbone exists mainly in an all-trans zig-zag conformation. To sum up, the participation of hydrocarbon chains in the surface potential change of phosphatidylcholines is mainly steric, related to packing density and order, which is in agreement with previous work [43].

In the next step of our studies, we examined the influence of the interfacial area and polar group modification on surface potential isotherms (Figure 3).
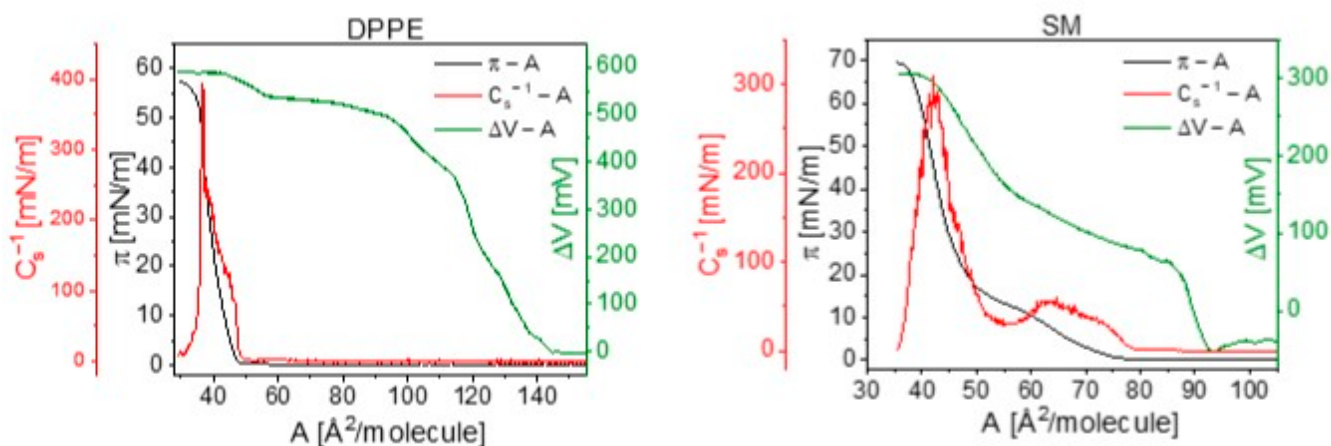

Figure 3. Electric surface potential change and surface pressure isotherms, together with calculated compressional moduli curves for (**A**) DPPE and (**B**) SM.

The SM molecule contains the same polar group as the PCs (the phosphocholine group), however, its structure is different in the region of the sphingosine backbone. The π–A and ΔV–A isotherms measured for SM show an analogical course to DPPC and suggest the existence of stable liquid-expanded and liquid-condensed phases. Despite this fact, the values of the critical area (92.9 Å^2 per molecule) and the maximum of surface potential (295 mV) for SM are significantly lower than for DPPC. Values read from the measured ΔV–A isotherm of SM are in agreement with the literature [24].

In the next part of our studies, we examined the electrical properties of monolayers composed of a representative of phosphatidylethanolamines—DPPE. The ΔV–A curve is characterized by a gradual increase, without any visible inflections, starting from molecular area 144 Å^2 and reaching a maximum value of surface potential equal to 573 mV (in agreement with the literature data, reporting values ranging from 520 mV [18] to 589 mV [23]).

To enrich and interpret the results obtained from our experiments, theoretical DFT calculations of molecular conformations were performed. The values of the total dipole moments of free molecules in a vacuum (μ_{tot}) are compiled in Table 2. To determine the magnitude of the normal component of the electrical dipole moment, μ_z, two different approaches were applied. Firstly, the values μ_z were directly read from the total dipole moment μ_{tot} of the molecule in a vacuum ($\varepsilon = 1$). Additionally, the component of the dipole moment in the plane of the interface (μ_{x-y}) has also been provided. However, it should be emphasized that the calculated dipole moment corresponds to the free molecule, and not to the molecule adsorbed at the interface. Therefore μ_z cannot be directly compared to μ_A^{exp} values obtained from experimental ΔV–A dependencies. In this approach, the molecule is treated as a single entity, without distinguishing its local parts (polar/apolar). As a result, differences in dielectric permittivity between polar and apolar parts are not taken into consideration. In the second approach, we separated the normal component of the dielectric dipole moment of a free molecule into contributions from the polar head ($\mu_\perp^p$) and hydrocarbon chains ($\mu_\perp^a$) individually (see Figure 4). The results of these theoretical calculations (μ_{tot}, μ_{x-y}, μ_z, $\mu_\perp^p$, $\mu_\perp^a$) are collected in Table 2.

In the next step of our calculations, we were interested in relating theoretical and experimental values, using the following equation [16], introducing the values of local dielectric permittivities (ε_p, ε_a) to the theoretically calculated normal dipole moments of

the polar and apolar groups ($\mu_\perp^p$, $\mu_\perp^a$) as well as the contribution from the reorientation of water molecules ($\mu_\perp^w / \varepsilon_w$):

$$\mu_A^{calc} = \frac{\mu_\perp^w}{\varepsilon_w} + \frac{\mu_\perp^p}{\varepsilon_p} + \frac{\mu_\perp^a}{\varepsilon_a} \tag{4}$$

In Equation (4), there are three unknown parameters: ($\mu_\perp^w / \varepsilon_w$), ε_p and ε_a. Therefore, initially, we took these values from other works [16,18,19] to see which set of values best fits the value μ_A^{exp} obtained experimentally. The obtained results are presented in Table 3.

Table 2. Values of dipole moments and their contributions, calculated using Gaussian software for entire molecules and their selected parts in vacuum.

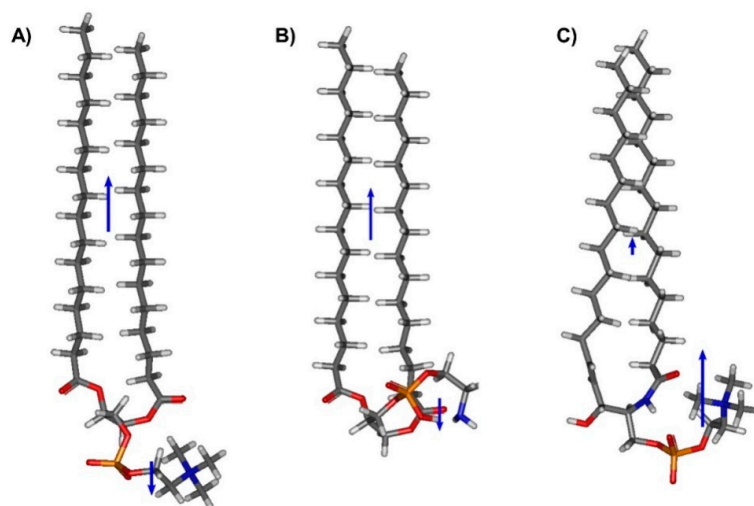| Phospholipid	Molecular Dipole Moment in Vacuum (D)			Group Dipole Moment (D)	
	μ_{tot}	μ_{x-y}	μ_z	$\mu_\perp^p$	$\mu_\perp^a$
DPPC	13.07	13.05	0.66	−1.89	2.55
DSPC	13.01	13.00	0.55	−2.16	2.71
DAPC	13.07	13.02	1.06	−1.43	2.49
DOPC	13.04	11.88	5.39	3.40	1.99
DPPE	8.63	8.57	0.94	−1.00	1.94
SM	14.33	9.94	10.33	10.30	0.03

Figure 4. Molecular structure of selected phospholipids: DPPC (**A**), DPPE (**B**) and SM (**C**) with the directions of normal components of electrical dipole moment visualized separately for the polar group ($\mu_\perp^p$) and hydrocarbon chains ($\mu_\perp^a$). Carbon atoms are visualized in dark gray, hydrogen in bright gray, oxygen in red, nitrogen in blue and phosphorus in orange.

As can be seen, the results obtained using the literature values of parameters do not agree with the experimentally determined μ_A^{exp}. Therefore, in the second step, we developed a new methodology. For a series of phosphatidylcholines DPPC, DSPC, DAPC and DOPC, multiple linear regression was used to find a model describing the relationship between the normal components of the calculated dipole moments of the polar and apolar parts of molecules and their experimental values $\left(\mu_A^{exp} \right)$. The equation of the fitted model has the following form:

$$\mu_A^{calc(4)} = -1.8 + 0.098 \cdot \mu_\perp^p + 1.05 \cdot \mu_\perp^a \tag{5}$$

which means that the determined parameters are equal to: $\mu_\perp^w / \varepsilon_w = -1.8 \pm 1.4 \ D$; $\varepsilon_p = 10.2 \pm 7.0$ and $\varepsilon_a = 0.95 \pm 0.52$. The predicted parameters show good agreement with

the observed parameters, as shown in Figure 5. The R-squared statistic indicates that the fitted model explains 86% of the variability in μ_A.

Table 3. Values of apparent dipole moments calculated from Equation (4) using the set of values of $(\mu_{\perp}^w/\varepsilon_w)$, ε_p and ε_a equal to (1) 0.04; 7.6 and 5.3 (according to [16]); (2) −0.065; 6.4 and 2.8 (according to [18]); (3) 0.04; 7.6; 4.2 (according to [19]); (4) −1.8; 10.2; 0.95 (according to our model).

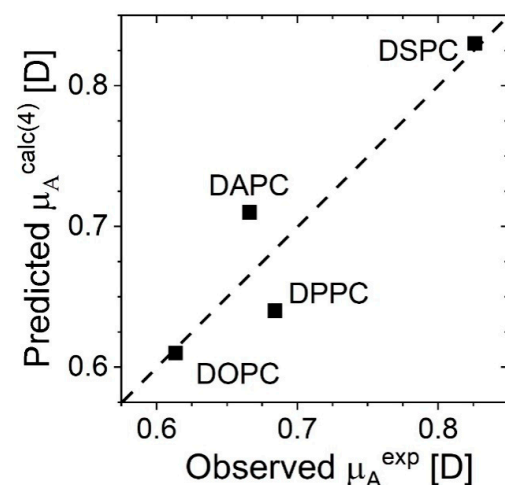| Phospholipid	Apparent Dipole Moment (D)			
	$\mu_A^{calc(1)}$	$\mu_A^{calc(2)}$	$\mu_A^{calc(3)}$	$\mu_A^{calc(4)}$
DPPC	0.32	0.60	0.44	0.68
DSPC	0.27	0.57	0.40	0.83
DAPC	0.27	0.55	0.40	0.67
DOPC	0.86	1.18	0.96	0.61
DPPE	0.27	0.47	0.37	0.13
SM	1.40	1.55	1.40	−0.78

Figure 5. Predicted $\mu_A^{calc(4)}$ versus experimental μ_A^{exp} values for the studied phosphatidylcholines with the line of identity.

As can be seen, the second value (ε_a) is about ten times smaller compared to ε_p, which indicates that the contribution of non-polar groups to the apparent dipole moment is more significant. A similar relationship was found by other authors [16,18,19], however, this effect was not so pronounced. This can result from the fact that literature models were based on homological series of compounds with small, simple polar groups (such as −COOH, −OH, −NH$_2$), whereas our approach involves bulky, zwitterionic systems. The obtained contribution from the reorientation of water molecules $\mu_{\perp}^w/\varepsilon_w$ is high, which can be explained by the ability of phosphatidylcholines to form hydrogen bonds with surrounding water dipoles. It is known that the hydration of the polar PC head groups is very high (even 11 water molecules per DPPC [44]), which may result in the formation of an organized water "quasi ice" lattice in the vicinity of a phosphocholine moiety [45]. The model developed in this paper for phosphatidylcholines cannot be applied to other phospholipids due to different hydration of polar groups (i.e., hydration for PC was determined to be 11.3 water molecules per lipid, whereas for PE it is 6.6). Although SM possesses the same polar group as PC, the presence of the hydroxyl group in the interfacial region may affect its hydration [46].

4. Conclusions

In this work, a systematic study on the surface potentials of Langmuir monolayers formed by the most abundant mammalian membrane phospholipids was performed to determine the values of their apparent dipole moments and to propose an improved

protocol for estimating individual contributions to a three-layer capacitor model. Our methodology correlates the results from DFT molecular modeling with experimentally determined values using multiple linear regression. It can be applied to the study of other phosphatidylcholine derivatives (with similar hydration) with different hydrocarbon chain lengths and saturations. To be able to determine the parameters ($\mu_{\perp}^{w}/\varepsilon_{w}$), ε_{p} and ε_{a} for other kinds of phospholipids, a similar approach should be carried out for their homologous series.

Author Contributions: Conceptualization P.D.-L. and J.K.; investigation, A.C.-B. and J.K.; data curation and visualization, J.K., A.C.-B. and A.W.; manuscript writing P.D.-L., A.C.-B. and A.W. All authors have read and agreed to the published version of the manuscript.

Conflicts of Interest: The authors declare no conflict of interest regarding the publication of this article.

References

1. Barnes, G.; Gentle, I. *Interfacial Science: An Introduction*, 2nd ed.; Oxford University Press: Oxford, UK, 2011; ISBN 9780199571185.
2. Daear, W.; Mahadeo, M.; Prenner, E.J. Applications of Brewster angle microscopy from biological materials to biological systems. *Biochim. Biophys. Acta Biomembr.* **2017**, *1859*, 1749–1766. [CrossRef] [PubMed]
3. Stottrup, B.L.; Nguyen, A.H.; Tüzel, E. Taking another look with fluorescence microscopy: Image processing techniques in Langmuir monolayers for the twenty-first century. *Biochim. Biophys. Acta Biomembr.* **2010**, *1798*, 1289–1300. [CrossRef] [PubMed]
4. Nobre, T.M.; Pavinatto, F.J.; Caseli, L.; Barros-Timmons, A.; Dynarowicz-Łatka, P.; Oliveira, O.N. Interactions of bioactive molecules & nanomaterials with Langmuir monolayers as cell membrane models. *Thin Solid Films* **2015**, *593*, 158–188.
5. Jaroque, G.N.; Sartorelli, P.; Caseli, L. The effect of the monocyclic monoterpene tertiary alcohol γ-terpineol on biointerfaces containing cholesterol. *Chem. Phys. Lipids* **2020**, *230*, 104915. [CrossRef]
6. Ceridório, L.F.; Caseli, L.; Oliveira, O.N. Chondroitin sulfate interacts mainly with headgroups in phospholipid monolayers. *Colloids Surf. B. Biointerfaces* **2016**, *141*, 595–601. [CrossRef]
7. Nakahara, H.; Hagimori, M.; Mukai, T.; Shibata, O. Monolayers of a tetrazine-containing gemini amphiphile: Interplays with biomembrane lipids. *Colloids Surf. B. Biointerfaces* **2018**, *164*, 1–10. [CrossRef]
8. Nakahara, H.; Hagimori, M.; Mukai, T.; Shibata, O. Interactions of a Tetrazine Derivative with Biomembrane Constituents: A Langmuir Monolayer Study. *Langmuir* **2016**, *32*, 6591–6599. [CrossRef]
9. Dynarowicz, P. Recent developments in the modeling of the monolayers structure at the water/air interface. *Adv. Colloid Interface Sci.* **1993**, *45*, 215–241. [CrossRef]
10. Oliveira, O.N.; Bonardi, C. The Surface Potential of Langmuir Monolayers Revisited. *Langmuir* **1997**, *13*, 5920–5924. [CrossRef]
11. Adam, N.K.; Danielli, J.F.; Harding J., B. The structure of surface films XXI—Surface potentials of dibasic esters, alcohols, aldoximes, and ketones. *Proc. Math. Phys. Eng. Sci.* **1934**, *147*, 491–499.
12. Schuhmann, D. Electrical properties of adsorbed or spread films: The effective value of permittivities in the Helmholtz equation (plane distribution of point dipoles). *J. Colloid Interface Sci.* **1990**, *134*, 152–160. [CrossRef]
13. Broniatowski, M.; Macho, I.S.; Miñones, J.; Dynarowicz-Łatka, P. Langmuir monolayers characteristic of (Perfluorodecyl)-alkanes. *J. Phys. Chem. B.* **2004**, *108*, 13403–13411. [CrossRef]
14. Shibata, O.; Krafft, M.P. Mixed Langmuir monolayers made from single-chain perfluoroalkylated amphiphiles. *Langmuir* **2000**, *16*, 10281–10286. [CrossRef]
15. Oliveira, O.N.; Taylor, D.M.; Morgan, H. Modelling the surface potential-area dependence of a stearic acid monolayer. *Thin Solid Films* **1992**, *210–211*, 76–78. [CrossRef]
16. Demchak, R.J.; Fort, T. Surface dipole moments of close-packed un-ionized monolayers at the air-water interface. *J. Colloid Interface Sci.* **1974**, *46*, 191–202. [CrossRef]
17. Dynarowicz, P.; Paluch, M. Electrical properties of some adsorbed films at the water-air interface. *J. Colloid Interface Sci.* **1985**, *107*, 75–80. [CrossRef]
18. Oliveira, O.N.; Taylor, D.M.; Lewis, T.J.; Salvagno, S.; Stirling, C.J.M. Estimation of group dipole moments from surface potential measurements on Langmuir monolayers. *J. Chem. Soc. Faraday Trans. 1 Phys. Chem. Condens. Phases* **1989**, *85*, 1009–1018. [CrossRef]
19. Petrov, J.G.; Polymeropoulos, E.E.; Möhwald, H. Three-capacitor model for surface potential of insoluble monolayers. *J. Phys. Chem.* **1996**, *100*, 9860–9869. [CrossRef]

20. Mozaffary, H. On the sign and origin of the surface potential of phospholipid monolayers. *Chem. Phys. Lipids* **1991**, *59*, 39–47. [CrossRef]
21. Beitinger, H.; Vogel, V.; Möbius, D.; Rahmann, H. Surface potentials and electric dipole moments of ganglioside and phospholipid monolayers: Contribution of the polar headgroup at the water/lipid interface. *Biochim. Biophys. Acta Biomembr.* **1989**, *984*, 293–300. [CrossRef]
22. Smaby, J.M.; Brockman, H.L. Surface dipole moments of lipids at the argon-water interface. Similarities among glycerol-ester-based lipids. *Biophys. J.* **1990**, *58*, 195–204. [CrossRef]
23. Nakahara, H.; Nakamura, S.; Nakamura, K.; Inagaki, M.; Aso, M.; Higuchi, R.; Shibata, O. Cerebroside Langmuir monolayers originated from the echinoderms: I. Binary systems of cerebrosides and phospholipids. *Colloids Surf. B. Biointerfaces* **2005**, *42*, 157–174. [CrossRef] [PubMed]
24. Sakamoto, S.; Nakahara, H.; Shibata, O. Miscibility behavior of sphingomyelin with phytosterol derivatives by a Langmuir monolayer approach. *J. Oleo Sci.* **2013**, *62*, 809–824. [CrossRef] [PubMed]
25. Frisch, M.J.; Trucks, G.W.; Schlegel, H.B.; Scuseria, G.E.; Robb, M.A.; Cheeseman, J.R.; Scalmani, G.; Barone, V.; Petersson, G.A.; Nakatsuji, H.; et al. *Gaussian 16, Revision B.01*; Gaussian Inc.: Wallingford, CT, USA, 2016.
26. Becke, A.D. Density-functional thermochemistry. III. The role of exact exchange. *J. Chem. Phys.* **1993**, *98*, 5648–5652. [CrossRef]
27. Lee, C.; Yang, W.; Parr, R.G. Development of the Colle-Salvetti correlation-energy formula into a functional of the electron density. *Phys. Rev. B.* **1988**, *37*, 785–789. [CrossRef]
28. Vosko, S.H.; Wilk, L.; Nusair, M. Accurate spin-dependent electron liquid correlation energies for local spin density calculations: A critical analysis. *Can. J. Phys.* **1980**, *58*, 1200–1211. [CrossRef]
29. Stephens, P.J.; Devlin, F.J.; Chabalowski, C.F.; Frisch, M.J. Ab Initio Calculation of Vibrational Absorption and Circular Dichroism Spectra Using Density Functional Force Fields. *J. Phys. Chem.* **1994**, *98*, 11623–11627. [CrossRef]
30. McLean, A.D.; Chandler, G.S. Contracted Gaussian basis sets for molecular calculations. I. Second row atoms, Z = 11–18. *J. Chem. Phys.* **1980**, *72*, 5639–5648. [CrossRef]
31. Krishnan, R.; Binkley, J.S.; Seeger, R.; Pople, J.A. Self-consistent molecular orbital methods. XX. A basis set for correlated wave functions. *J. Chem. Phys.* **1980**, *72*, 650–654. [CrossRef]
32. Grimme, S.; Antony, J.; Ehrlich, S.; Krieg, H. A consistent and accurate ab initio parametrization of density functional dispersion correction (DFT-D) for the 94 elements H-Pu. *J. Chem. Phys.* **2010**, *132*, 154104. [CrossRef]
33. Stefaniu, C.; Brezesinski, G.; Möhwald, H. Polymer-capped magnetite nanoparticles change the 2D structure of DPPC model membranes. *Soft Matter* **2012**, *8*, 7952–7959. [CrossRef]
34. Kilic, S.; Bolukcu, E.S. Phase behavior of DSPC/PEG40St mixtures at higher emulsifier contents. *Colloids Surf. B. Biointerfaces* **2018**, *171*, 368–376. [CrossRef]
35. Borden, M.A.; Pu, G.; Runner, G.J.; Longo, M.L. Surface phase behavior and microstructure of lipid/PEG-emulsifier monolayer-coated microbubbles. *Colloids Surf. B Biointerfaces* **2004**, *35*, 209–223. [CrossRef] [PubMed]
36. Raju, R.; Torrent-Burgués, J.; Bryant, G. Interactions of cryoprotective agents with phospholipid membranes—A Langmuir monolayer study. *Chem. Phys. Lipids* **2020**, *231*, 104949. [CrossRef] [PubMed]
37. Korchowiec, B.; Paluch, M.; Corvis, Y.; Rogalska, E. A Langmuir film approach to elucidating interactions in lipid membranes: 1,2-dipalmitoyl-sn-glycero-3-phosphoethanolamine/cholesterol/metal cation systems. *Chem. Phys. Lipids* **2006**, *144*, 127–136. [CrossRef] [PubMed]
38. Wnętrzak, A.; Makyła-Juzak, K.; Filiczkowska, A.; Kulig, W.; Dynarowicz-Latka, P. Oxysterols Versus Cholesterol in Model Neuronal Membrane. I. The Case of 7-Ketocholesterol. The Langmuir Monolayer Study. *J. Membr. Biol.* **2017**, *250*, 553–564. [CrossRef] [PubMed]
39. Davies, J.T.; Rideal, E.K. *Interfacial phenomena*; Academic Press: Cambridge, MA, USA, 1963; ISBN 9780123956095.
40. Gragson, D.E.; Beaman, D.; Porter, R. Using compression isotherms of phospholipid monolayers to explore critical phenomena. A biophysical chemistry experiment. *J. Chem. Educ.* **2008**, *85*, 272–275. [CrossRef]
41. Taylor, D.M.; De Oliveira, O.N.; Morgan, H. Models for interpreting surface potential measurements and their application to phospholipid monolayers. *J. Colloid Interface Sci.* **1990**, *139*, 508–518. [CrossRef]
42. Sanchez, J.; Badia, A. Spatial variation in the molecular tilt orientational order within the solid domains of phase-separated, mixed dialkylphosphatidylcholine monolayers. *Chem. Phys. Lipids* **2008**, *152*, 24–37. [CrossRef]
43. Peterson, U.; Mannock, D.A.; Lewis, R.N.A.H.; Pohl, P.; McElhaney, R.N.; Pohl, E.E. Origin of membrane dipole potential: Contribution of the phospholipid fatty acid chains. *Chem. Phys. Lipids* **2002**, *117*, 19–27. [CrossRef]
44. Pasenkiewicz-Gierula, M.; Baczynski, K.; Markiewicz, M.; Murzyn, K. Computer modelling studies of the bilayer/water interface. *Biochim. Biophys. Acta Biomembr.* **2016**, *1858*, 2305–2321. [CrossRef] [PubMed]
45. Disalvo, E.A.; Lairion, F.; Martini, F.; Almaleck, H.; Diaz, S.; Gordillo, G. Water in biological membranes at interfaces: Does it play a functional role? *An. des la Asoc. Quim. Argentina* **2004**, *92*, 1–22.
46. Kodama, M.; Abe, M.; Kawasaki, Y.; Hayashi, K.; Ohira, S.; Nozaki, H.; Katagiri, C.; Inoue, K.; Takahashi, H. Estimation of interlamellar water molecules in sphingomyelin bilayer systems studied by DSC and X-ray diffraction. *Thermochim. Acta* **2004**, *416*, 105–111.